CONF-890748--4

Novel Applications of the Field Ion Microscope and Atom-Probe

SAND--89-0589C
DE89 008684

G. L. Kellogg

Introduced in 1951 and 1966 respectively, the field ion microscope[1] and atom-probe[2] mass spectrometer can hardly be considered new or emerging microprobes. Over the years, the ability to use these instruments to examine the structure and composition of various materials at the atomic level has been well established.[3-12] However, recent advances in more conventional microanalytical techniques, particularly progress towards a higher degree of spatial resolution, has created renewed interest in all techniques capable of analysis on a very fine scale. Also, there has been an increased emphasis over the past several years in the application of the field ion microscope and atom-probe to problems of greater general interest in surface and materials science. It is therefore not totally inappropriate to discuss the field ion microscope and atom-probe within the context of "emerging" microprobes. The intent of this paper is to familiarize the reader with the techniques of field ion microscopy and atom-probe mass spectroscopy and describe several recent applications which demonstrate some of their unique attributes.

Field Ion Microscopy

Conceptually, the field ion microscope is a very simple instrument. Shown schematically in Fig. 1, the microscope consists of a cryogenically cooled sample "tip" placed opposite to a fluorescent screen in an ultrahigh vacuum chamber. In addition, modern-day field ion microscopes almost

---

The author is at Sandia National Laboratories, Albuquerque, NM. This work was supported by the U. S. Department of Energy under contract DE-AC04-76DP00789

---

always include a channel plate next to the fluorescent screen for image intensification[7] (not shown in the figure). An image of the surface atoms at the apex of the tip is produced by the application of a high positive voltage (typically 5-20 kV) to the tip in the presence of an imaging gas such as He, Ne, or Ar. The extremely high electric field (of the order of tens of volts per nanometer) caused by the applied voltage ionizes the imaging gas atoms in a region directly above the protruding surface atoms. The positive ions formed in this process are accelerated away from the positively charged tip and travel to the screen where they form image spots. Because the ions are created preferentially above the protruding surface atoms, the pattern of spots which appears on the fluorescent screen is a direct image of those atoms. The magnification of the field ion microscope, given roughly by the ratio of the tip-to-screen distance to the tip radius, is of the order of several million. The resolution of the field ion microscope is a function of tip temperature and is sufficient to resolve individual atoms when the tip is at cryogenic temperatures.

Figure 2 shows an example of a field-ion-microscope image taken from a rhodium sample. The dark, circular regions seen in the image correspond to the flat, low-index planes of the surface. These regions are dark because the atoms within the plane do not protrude sufficiently to cause a local enhancement of the electric field. The rings of spots surrounding the dark regions correspond to the atoms at the edges of individual atomic layers. The smallest diameter ring corresponds to the edge of the topmost atomic layer and successively larger rings correspond to the edges of successively deeper atomic layers.

If the applied voltage to the tip is increased beyond that which produces a stable field-ion-microscope image, the electric field at the

surface becomes high enough to ionize and remove the surface atoms themselves. This process is known as either field evaporation or field desorption.[3-7] In the region of low-index planes field evaporation removes the substrate atoms from the edge of the plane inward, one layer at a time. The field evaporation process is very useful as the final step of sample preparation before field-ion imaging because it produces a surface which is free of contaminants and is smooth on an atomic scale. Field evaporation is also routinely used to probe into the near-surface region of the tip to find structural defects which may not extend to the initial surface.

As described later, the field ion microscope can be used in combination with the atom-probe mass spectrometer to gain information on the chemical composition as well as the atomic structure of the surface and near-surface region of a solid sample. However, even by itself, the field ion microscope continues to make contributions in various scientific disciplines. For example, one of its most unique applications has been the investigation of the diffusion and interaction of individual surface atoms. Pioneered by Ehrlich and co-workers,[13] these studies have provided quantitative diffusion parameters and interaction potentials for a variety of adsorbate substrate systems.[14-17] The field ion microscope has also made many significant contributions in the areas of metallurgy and materials science. For more information on these applications, the interested reader is referred to several review articles.[8-11]

In this report two examples of applications in the area of surface science will be described. The first involves the reconstruction of clean metal surfaces. It has been well established by low energy electron diffraction (LEED), ion scattering, and other techniques that the atomic structure of a single-crystal surface may differ from a simple termination

of the bulk structure.[18] Yet, the detailed arrangement of surface atoms is often difficult to discern from these techniques. An example is the (110) surfaces of Pt, Ir, and Au. The (110) surface of these fcc materials consists of close-packed rows of atoms aligned along the $[1\bar{1}0]$ direction. Investigations by LEED have shown very clearly that the atoms in the topmost (110) layer of Pt, Ir, and Au are rearranged with respect to the bulk and have a (1x2) periodicity.[18] This periodicity means that atoms along the rows have the same atomic spacing as atoms in the bulk, but the spacing between rows is twice that of the bulk. In the particular case of Pt, although all investigators agree on the (1x2) periodicity, there has been considerable controversy over the exact atomic arrangement giving rise to this periodicity.[18]

As indicated in Fig. 3, investigations with the field ion microscope have shown unambiguously that the (1x2) periodicity of the reconstructed Pt(110) surface is due to alternate missing rows of atoms.[19] Fig. 3(a) shows an image of a field-evaporated Pt surface in the vicinity of the (110) plane. The arrows indicate the direction of one of the close-packed rows of atoms in the topmost (110) layer. From the edge atoms of the underlying layer it is possible to determine that the rows of atoms in this field-evaporated surface lie in adjacent channels of the next layer down, i.e., the surface is not reconstructed. The ability to produce atomically perfect, unreconstructed surfaces by low-temperature field evaporation is a particularly useful feature of the field ion microscope for the investigation of surface reconstructions at the atomic level. Fig. 3(b) shows an image of the same surface after it had been heated to 330 K for one minute. During the heating interval the applied voltage was turned off to avoid any influence of the electric field on the reconstruction process.

Careful analysis of this image along with slow field evaporation of the topmost layer indicate that the rows of atoms in Fig. 3(b) are in every other channel of the underlying surface. The arrows point to an empty channel which was occupied by a row of atoms prior to the reconstruction. The arrangement of atoms in Fig. 3(b) corresponds to the so-called "missing-row" structure, which is now the accepted structure for Pt(110)(1x2). In similar experiments it was shown that the missing-row structure could be produced for as few as five atoms in the topmost layer indicating that the reconstruction is driven by short-ranged atomic interactions.[19] These types of investigations have now been extended to other reconstructed surfaces of Pt and Ir.[20-22] It has also been demonstrated that the field ion microscope can be used to investigate reconstructions of some of the higher index planes of Si[23] as well as adsorbate-induced reconstructions on Ni.[24]

The second application of the field ion microscope discussed in this article involves the nucleation of clusters on atomically perfect metal surfaces. Despite the fact that classical theories[25] of crystal growth either predict or assume that the growth of new atomic layers begins with a two-dimensional cluster nucleus, past observations with the field ion microscope have identified metal-metal overlayer systems in which the initial nucleus is a linear chain.[26-28] These chain nuclei are typically stable for clusters up to a critical number of atoms, beyond which two-dimensional islands are stable. On a W(110) substrate the critical number for Ni atoms is four, for Pd it is eight, for Ir it is approximately twelve, and for Pt stable chains of up to 24 atoms have been observed. It had been assumed that the asymmetry of the W(110) surface structure or the

difference in the size of the adsorbate atoms compared to the substrate atoms influenced the formation of the stable chain structures.

In more recent work it has been shown that chain nuclei can also occur in homogeneous nucleation on symmetric substrates.[29,30] For example, field ion microscope images of Ir atoms on an Ir(100) surface have shown directly that chain configurations are stable for five or fewer atoms and two-dimensional island configurations are stable for six or more atoms.[29] Photographs which illustrate this interesting phenomenon are shown in Fig. 4. Fig. 4(a) shows the topmost layer of atoms on an Ir(100) surface after it had been field evaporated such that just six atoms remain. The six Ir atoms are arranged in a rectangular configuration reflecting the symmetry of the fcc(100) surface. The rectangular configuration is stable upon heating up to temperatures of 460 K. Above this temperature the island dissociates and the atoms migrate off the topmost plane. Fig. 4(b) shows the same cluster with one of the corner atoms removed by field evaporation. When this atomic cluster is heated to 450 K, the five atoms transform irreversibly to the linear chain shown in Fig. 4(c). This chain configuration is stable and does not transform back to the island with additional heating. However, if a sixth atom is added to the surface (from an external deposition source) and allowed to migrate to the end of the chain, the six-atom chain readily transforms back to a two-dimensional configuration.[29] These experiments clearly demonstrate the stability of five-atom chains and six-atom islands. Additional experiments demonstrate the stability of three- and four-atom chains and islands larger than six atoms. The stability of these atomic clusters is now being used to determine the relative strengths of adatom-adatom bonds on single-crystal surfaces. Models based on a two-dimensional lattice gas indicate that

interactions extending to second-nearest neighbors are required for the chain nuclei to occur which suggests the presence of relatively long-ranged interactions in cluster nucleation on this surface.[31]

In similar investigations it has been shown that Pt adatom clusters on the Pt(100) surface actually oscillate between stable chain and island structures as the number of atoms is increased from two to six, i.e., chain configurations are stable for three and five atoms, whereas island configurations are stable for four, six, and more atoms.[30] The stability of these structures is predicted by calculations based on the Embedded Atom Method if lattice relaxations are included in the model. The calculations point to the strong repulsive interaction between atoms at the next-nearest separation and the surprisingly large four-body attractive interaction as the interactions which are responsible for driving these unusual oscillations.

Atom-Probe Mass Spectroscopy

The field ion microscope is primarily a probe of atomic structure. Chemical identification of species on the surface of a field ion tip became possible with the introduction of the atom-probe field ion microscope[2] or atom-probe, for short. This instrument combines a conventional field ion microscope with a sensitive time-of-flight mass spectrometer. In the most commonly used design, shown schematically in Fig. 5, a small hole is placed in the viewing screen of a field ion microscope and a detector, sensitive to the impact of individual ions, is placed at the end of a drift tube positioned behind the probe hole. The tip is externally adjusted to align an atom or group of atoms of interest with the probe hole. Surface atoms are removed (field evaporated) as positive ions by the application of a short-duration (10-100 ns), high voltage (0.5-3 kV) pulse superimposed on

the dc imaging voltage. The ions of interest travel through the probe hole to the detector. From the measured flight time of the ions and the known length of the drift tube it is a simple calculation to determine the mass-to-charge ratio of the field evaporated ions. If the tip is pulsed repetitively with the probe-hole over a given area of the surface, the chemical composition of a small volume of the sample can be determined. It is common to plot out the compositions as histograms of field-evaporated species. An example of such a histogram from a sample of $YBa_2Cu_3O_{7-x}$ is shown in Fig. 6 (from Ref. 32). Because chemical analysis in the atom-probe can be made specific to a given region, e.g., near an extended defect, the probe-hole type of atom-probe is well suited for the investigations of metallurgical problems such as impurity segregation to grain boundaries and other defects.[8-11] It should also be noted that a significant increase in mass resolution can be achieved with the use of an energy-focussing lens in place of the straight, drift tube.[33] With the energy-focussed atom-probe the isotopes of all commonly studied materials can be resolved.

One disadvantage of the probe-hole atom-probe is that the majority of species which are field evaporated from the surface do not pass through the probe-hole and are not detected. Studies of surface adsorption and reaction processes may therefore require many cycles of dosing and desorption to obtain statistically significant surface compositions. This problem can be addressed with a different type of atom-probe known as the imaging atom-probe.[34] A schematic diagram of the imaging atom-probe is shown in Fig. 7. In this instrument the viewing screen of the field ion microscope is an imaging detector sensitive to the impact of single ions. Each ion which strikes the front surface of the detector produces a current

pulse which is amplified and displayed on the sweep of a fast waveform digitizer. The detector also displays an image spot at the position of ion impact. Surface species field desorbed from anywhere on the imaged portion of the surface are detected and identified by their flight times. Although the increased signal makes the imaging atom-probe better suited to the study of surface adsorption processes, its shorter flight path results in significantly poorer mass resolution. An additional feature of the imaging atom-probe is the ability to obtain elemental maps of selected surface species.[34] These maps are obtained by switching on the detector during the arrival time of a given species. The transient image of spots appearing on the detector, which corresponds to the selected species only, can be photographically recorded. The "time-gated" image can then be superimposed on a field-ion image taken with the same detector at reduced gain to determine where on the surface the selected species originated.

Another type of atom-probe, known as the pulsed-laser atom-probe,[35,36] has greatly facilitated atom-probe investigations of semiconductors and insulators. In the pulsed-laser atom-probe a short-duration (0.1 - 10 ns) laser pulse is applied to a tip which is simultaneously subjected to a dc applied voltage. The combination of the thermal stimulation produced by the laser pulse and the high electric field provided by the applied voltage initiates field desorption. Time-of-flight mass analysis is carried out the same way as in either the probe-hole or imaging atom-probe. The use of laser pulses permits analysis of high resistivity materials which will not transmit the high-voltage electrical pulses. Elimination of the high voltage pulses also leads to a significant improvement in mass resolution. In addition, it has also been shown that the pulsed-laser atom-probe is useful for the investigation of a variety of surface reaction and

desorption phenomena. A recent review of the pulsed-laser atom-probe can be found in the literature.[37]

The atom-probe field ion microscope has been applied to a variety of problems in a wide range of scientific disciplines. Discussions of these applications can be found in a number of review articles.[6-12] Here, an example of how the atom-probe has been applied to the study of surface oxide formation is provided to illustrate the quantitative nature of the chemical analysis which can be performed. The formation of thin metal oxides is of considerable interest in research areas such as corrosion, catalysis, and adhesion. Metal oxides have also become important in microelectronics, where a need for very thin insulating materials has developed. Crucial to the characterization of thin metal oxides is the ability to determine the composition of the film from the surface through the metal-oxide interface. In the example presented here it is shown that this type of characterization is possible with the atom-probe.

The metal substrate used in this study was rhodium.[38] The choice of rhodium was motivated by its well-known catalytic properties and the influence of surface oxides on the catalytic activity.[39] The experimental apparatus consisted of two UHV chambers: a reaction chamber in which the rhodium tips were oxidized and an analysis chamber in which field ion microscopy and imaging atom-probe mass spectroscopy were carried out. A rhodium tip was first introduced into the analysis chamber and its surface was cleaned by neon ion bombardment and dc field evaporation. The atomic structure of the surface was examined by field ion microscopy. The sample tip was then transferred under ultrahigh vacuum to the reaction chamber where it was oxidized in 1 Torr O_2 at 600 K for 15 minutes. The oxygen was

removed from the reaction chamber and the tip was returned to the analysis chamber without exposure to air.

The composition of the oxide was examined in the analysis chamber. The oxide layer was removed by pulsed-voltage field evaporation and the desorbed species were mass analyzed. The primary species detected in the mass scans were atomic and molecular oxygen, water, and various charge states of rhodium and rhodium oxide. The layer was removed at a rate of about one layer per pulse with a total of 50-70 pulses used to remove the entire film. For these studies only a small region of the surface was probed to better examine the metal-oxide interface. This was accomplished by positioning a disk with a small aperture in front of the tip during analysis. The chemical composition of the oxide was obtained by plotting the cumulative number of oxygen atoms detected versus the cumulative number of rhodium atoms.

An example of such a cumulative plot is shown in Fig. 8. It is obvious from the graph that there are three distinct slopes in the plot. The initial slope is 3/2 indicating that the outer oxide is stoichiometric Rh_2O_3. This is the stable form of rhodium below 1023 K and has the corundum structure.[40] The thickness of the oxide film is estimated to be of the order of 50-60 layers. The next region has a slope varying from 0.3 to 0.5. This slope does not correspond to any expected suboxide and varies somewhat from experiment to experiment. Most likely the region contains a mixture of suboxides and dissolved oxygen and for that reason is labeled "dissolved oxygen." The thickness of the transition region is 5-15 Rh layers. The third region of the plot has slope 0 and corresponds to bulk Rh.

The results of the above investigation showed quite explicitly that thin oxide films grown on Rh at elevated temperatures consist of a single phase of Rh_2O_3. Moreover, it was discovered that the transition region from this oxide to the metal substrate is very narrow extending only a few atomic layers. This type of experiment clearly demonstrates that detailed information on the composition of thin oxide films can be obtained in controlled studies with the atom-probe. In additional studies it was shown that the growth law, the activation energy for oxygen uptake, and the conditions under which the Rh oxide layer could be removed by CO reduction can also be obtained in studies with the imaging atom-probe.[41] Similar experimental methods have been used to investigate oxide growth on other metal surfaces with atom-probe techniques.[9,43-45]

Summary

The unique attributes of the field ion microscope and atom-probe mass spectrometer permit structural and chemical analysis at the atomic level. In this paper a brief overview of the operating principles for the two instruments was given. In addition, three specific examples, which illustrate the type of analysis possible with the techniques, were discussed. These examples were chosen primarily based on the author's recent research interests. Many other applications which emphasize other novel aspects of the field ion microscope and atom-probe are reviewed in the literature.[3-12]

References

1. E. W. Müller, Z. Physik 131, 136 (1951).

2. E. W. Müller, J. A. Panitz, and S. B. McLane, Jr., Rev. Sci. Instrum. 39, 83 (1968).

3. J. J. Hren and S. Ranganathan, eds., Field Ion Microscopy (Plenum, New York, 1968).

4. E. W. Müller and T. T. Tsong, Field Ion Microscopy, Principles and Applications (Elsevier, New York, 1969).

5. K. M. Bowkett and D. A. Smith, Field Ion Microscopy (North Holland, Amsterdam-London, 1970).

6. E. W. Müller and T. T. Tsong, "Field Ion Microscopy, Field Ionization, and Field Evaporation," in Progress in Surface Science, ed. S. Davison, (Pergamon, New York, 1973) Vol. 1, Part 4.

7. J. A. Panitz, J. Phys. E: Sci. Instrum. 15, 1281 (1982).

8. S. S. Brenner, Surface Sci. 70, 427 (1978).

9. B. Ralph, S. A. Hill, M. J. Southon, M. P. Thomas, and A. R. Waugh, Ultramicroscopy 8, 361 (1982).

10. G. D. W. Smith, "Field Ion Microscopy and Atom-Probe Microanalysis," in Metals Handbook, ed. R. E. Whan, (Am. Soc. for Metals, Metals Park, OH, 1986) p. 583.

11. M. K. Miller, Materials Rev. 32, 221 (1987).

12. T. T. Tsong, Surface Sci. Reports, 8, 127 (1988).

13. G. Ehrlich and F. G. Hudda, J. Chem. Phys. 44, 1039 (1966).

14. G. L. Kellogg, T. T. Tsong, and P. L. Cowan, Surface Sci. 70, 485 (1978).

15. T. T. Tsong and P. L. Cowan, CRC Crit. Rev. Solid State Mater. Sci. 7, 289 (1978).

16. G. Ehrlich and K. Stolt, Ann. Rev. Phys. Chem. 31, 603 (1980).

17. D. W. Bassett, "Observing Surface Diffusion at the Atomic Level," in Surface Mobilities on Solid Materials, ed. V. T. Binh, (Plenum, New York, 1983) p. 63.

18. P. J. Estrup, "Reconstruction of Metal Surfaces," in Chemistry and Physics of Solid Surfaces, ed. R. Vanselow and R. Howe, (Springer-Verlag, Berlin, 1984) Vol. 5, p. 205.

19. G. L. Kellogg, Phys. Rev. Lett. 55, 2168 (1985).

20. J. Witt and K. Müller, Phys. Rev. Lett. 57, 1153 (1986).

21. Q. Gao and T. T. Tsong, Phys. Rev. B. 36, 2547 (1987).

22. G. L. Kellogg, J. Vac. Sci. Technol. A5, 747 (1987).

23. H. Liu, T. T. Tsong, and Y. Liou, Phys. Rev. Lett. 58, 1535 (1987).

24. G. L. Kellogg, Phys. Rev. B 37, 4288 (1988).

25. J. P. Hirth and G. M. Pound, "Condensation and Evaporation, Nucleation and Growth Kinetics, in Progress in Materials Science (Pergamon, New York, 1963) Vol. II

26. D. W. Bassett, Thin Solid Films 48, 237 (1978).

27. H. W. Fink and G. Ehrlich, Surface Sci. 110, L611 (1981).

28. P. R. Schwoebel and G. L. Kellogg, Phys. Rev. B 38, 5326 (1988).

29. P. R. Schwoebel and G. L. Kellogg, Phys. Rev. Lett. 61, 578 (1988).

30. P. R. Schwoebel, S. M. Foiles, C. L. Bisson, and G. L. Kellogg, Phys. Rev. Lett. (submitted for publication).

31. P. R. Schwoebel, P. J. Feibelman, and R. L. Schwoebel, Surface Sci. (submitted for publication).

32. S. S. Brenner and G. L. Kellogg, Proc. MRS Symposium on High -T_c Superconductors, Boston MA, 11/30-12/5, 1987.

33. E. W. Müller and S. V. Krishnaswami, Rev. Sci. Instrum. 45, 1053 (1974).

34. J. A. Panitz, Rev. Sci. Instrum. 44, 1043 (1973).

35. G. L. Kellogg and T. T. Tsong, J. Appl. Phys. 51, 1184 (1980).

36. W. Drachsel, S. Nishigaki, and J. H. Block, Int. J. Mass Spectrom. Ion Phys. 32, 333 (1980).

37. G. L. Kellogg, J. Phys. E: Sci. Instrum. 20, 125 (1987).

38. G. L. Kellogg, Appl. Phys. Lett. 51, 100 (1987).

39. G. L. Kellogg, J. Catal. 92, 167 (1985).

40. J. M. D. Coey, Acta Crystallogr. Sec. B 26, 1876 (1970).

41. G. L. Kellogg, Surface Sci. 171, 359 (1986).

42. Y. S. Ng, S. B. McLane. Jr., and T. T. Tsong, J. Appl. Phys. 49, 2517 (1978).

43. G. K. L. Cranstoun, D. R. Pyke, and G. D. W. Smith, Appl. Surface Sci. 2, 375 (1979).

44. K. Hono, T. Sakurai, and H. W. Pickering, J. de Physique (Paris), Colloque C6, Tome 48, 505 (1987).

45. Z. G. Liu, Y. Chen, and X. Z. Wen, Surface Sci. 208, L15 (1989).

Figure Captions

FIG. 1.--Schematic drawing of field ion microscope.

FIG. 2.--Helium field ion microscope image from Rh at 6.6 kV.

FIG. 3.--Field ion micrographs showing reconstruction of Pt(110). (a) unreconstructed surface (b) reconstructed to missing-row structure (from ref. 19).

FIG. 4.--Field ion micrographs showing the stability of Ir adatom clusters on Ir(100). (a) stable island of six atoms, (b) metastable island of five atoms produced by field evaporation of corner atom, (c) stable chain of five atoms produced by heating five-atom island (from ref. 29).

Fig. 5.--Schematic drawing of probe-hole atom-probe field ion microscope

Fig. 6.--Histogram of field evaporated ions from sample of $YBa_2Cu_3O_{7-x}$ (from ref. 32).

Fig. 7.--Schematic drawing of imaging atom-probe.

Fig. 8.--Cumulative plot of field desorbed oxygen atoms vs. field-desorbed rhodium atoms. Slope of plot identified chemical form of oxide (from ref. 38).

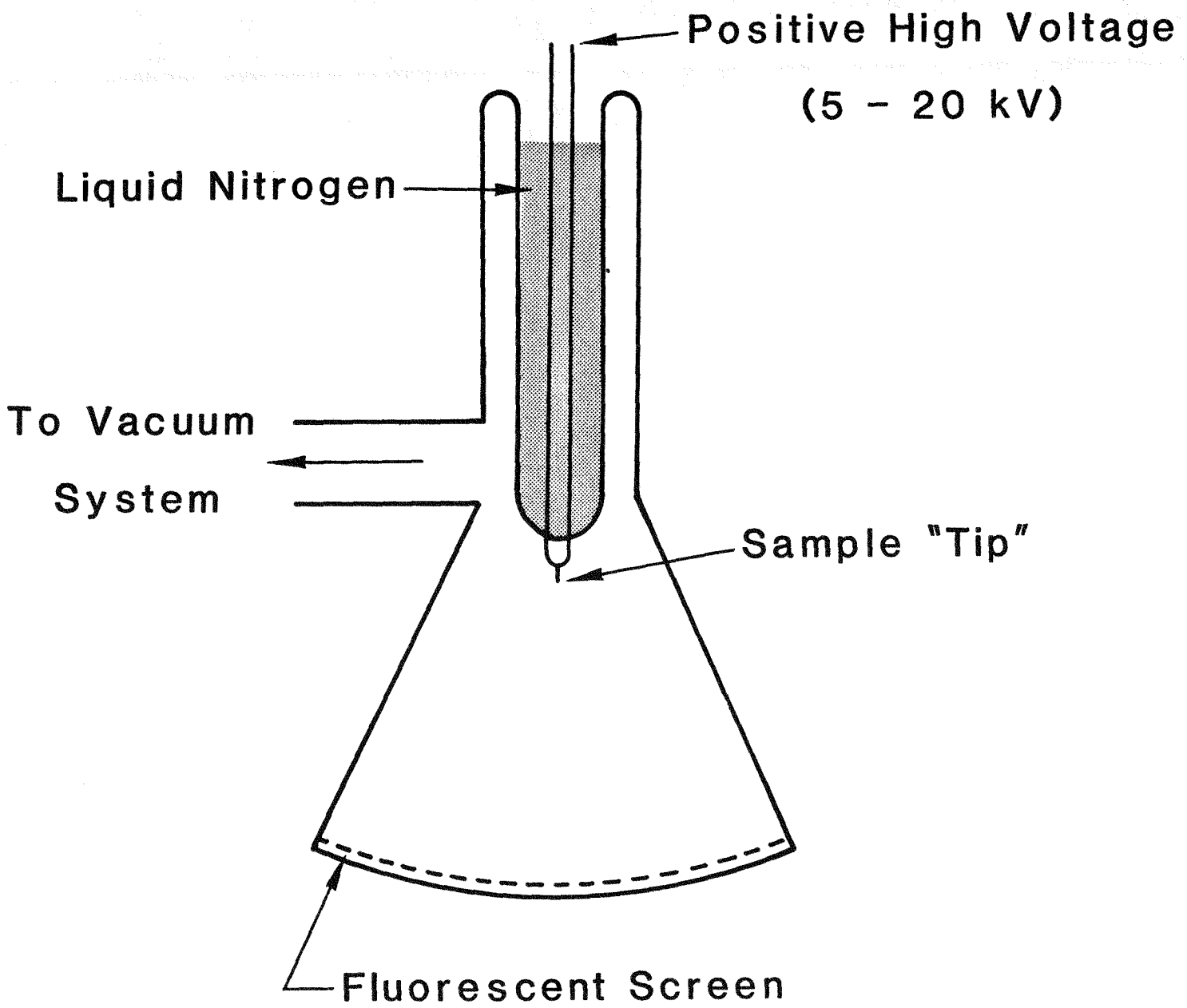
Positive High Voltage
(5 - 20 kV)
Liquid Nitrogen
To Vacuum
System
Sample "Tip"
Fluorescent Screen

Fig. 1

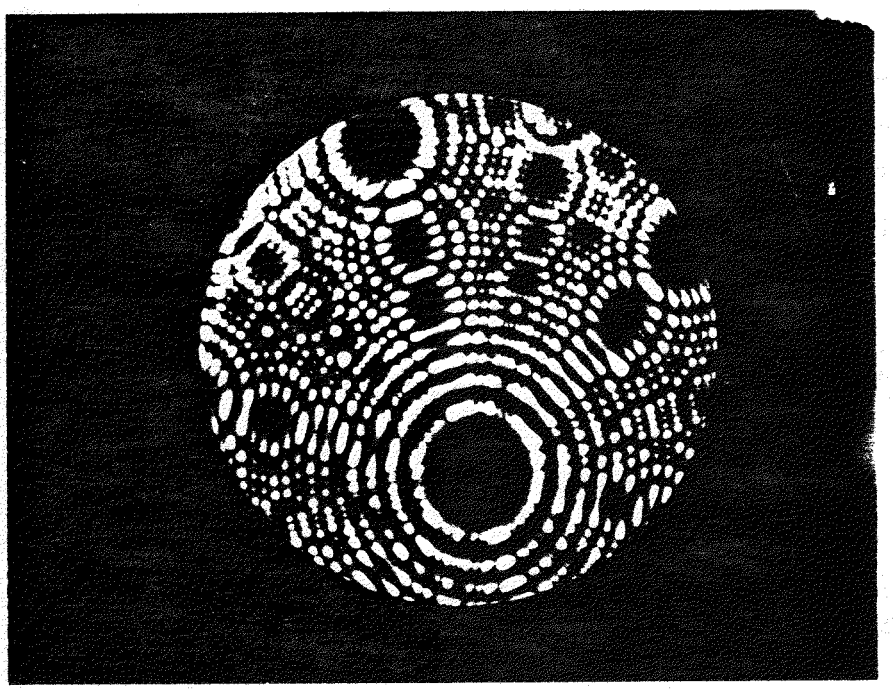

Fig. 2

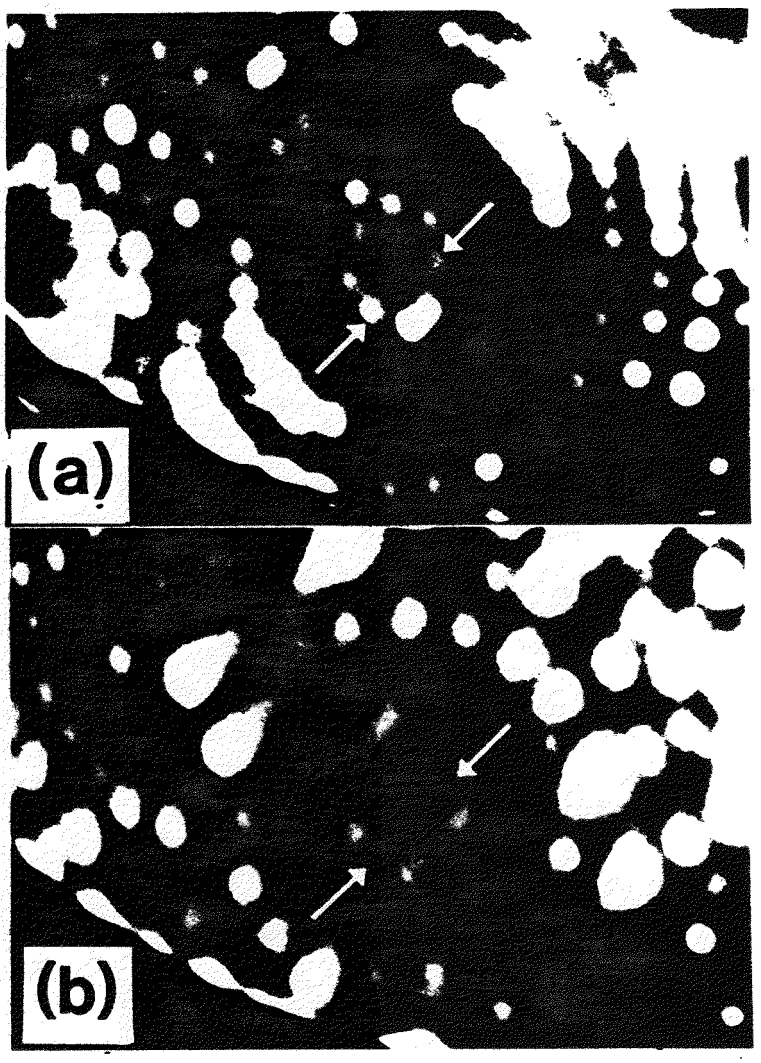

Fig. 3

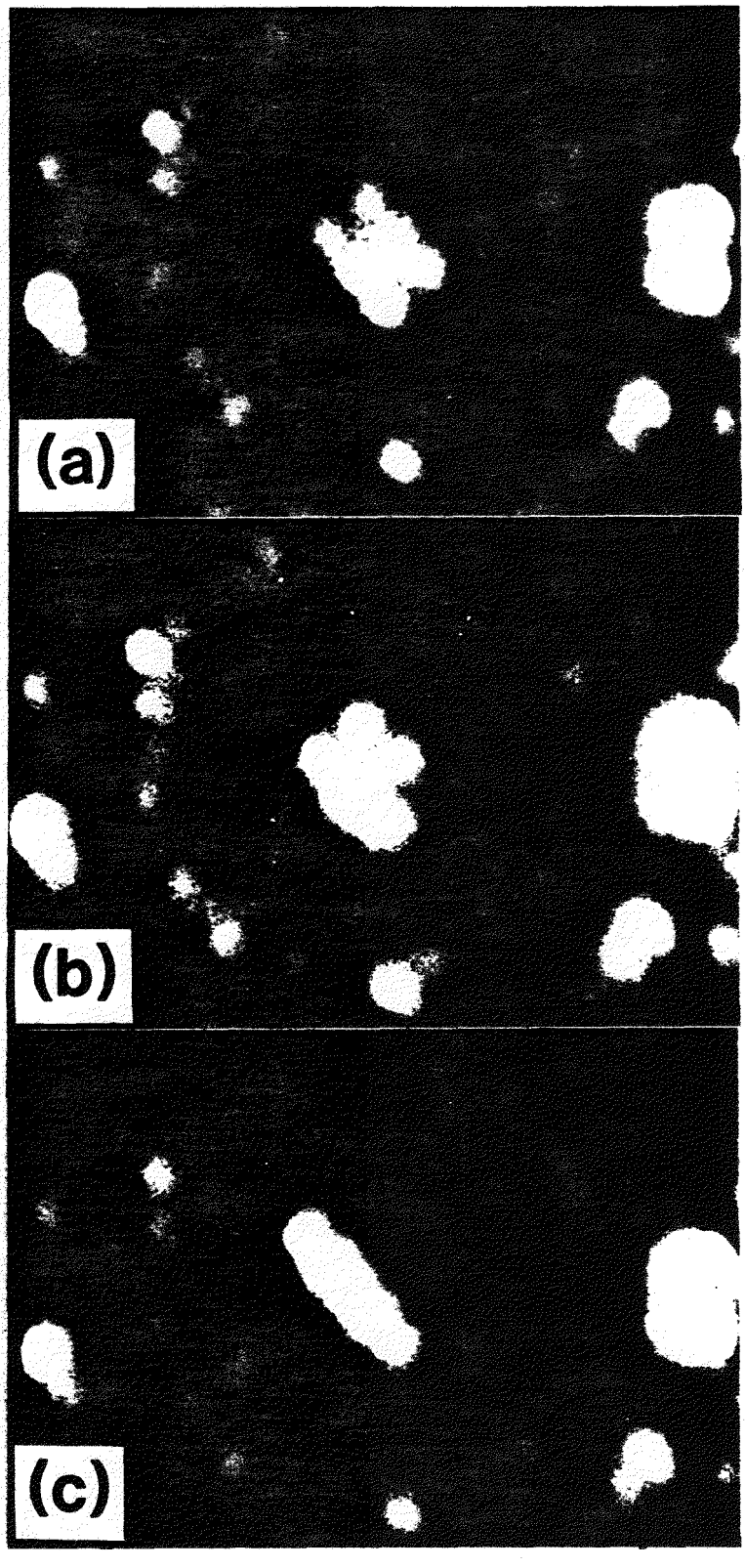

Fig. 4

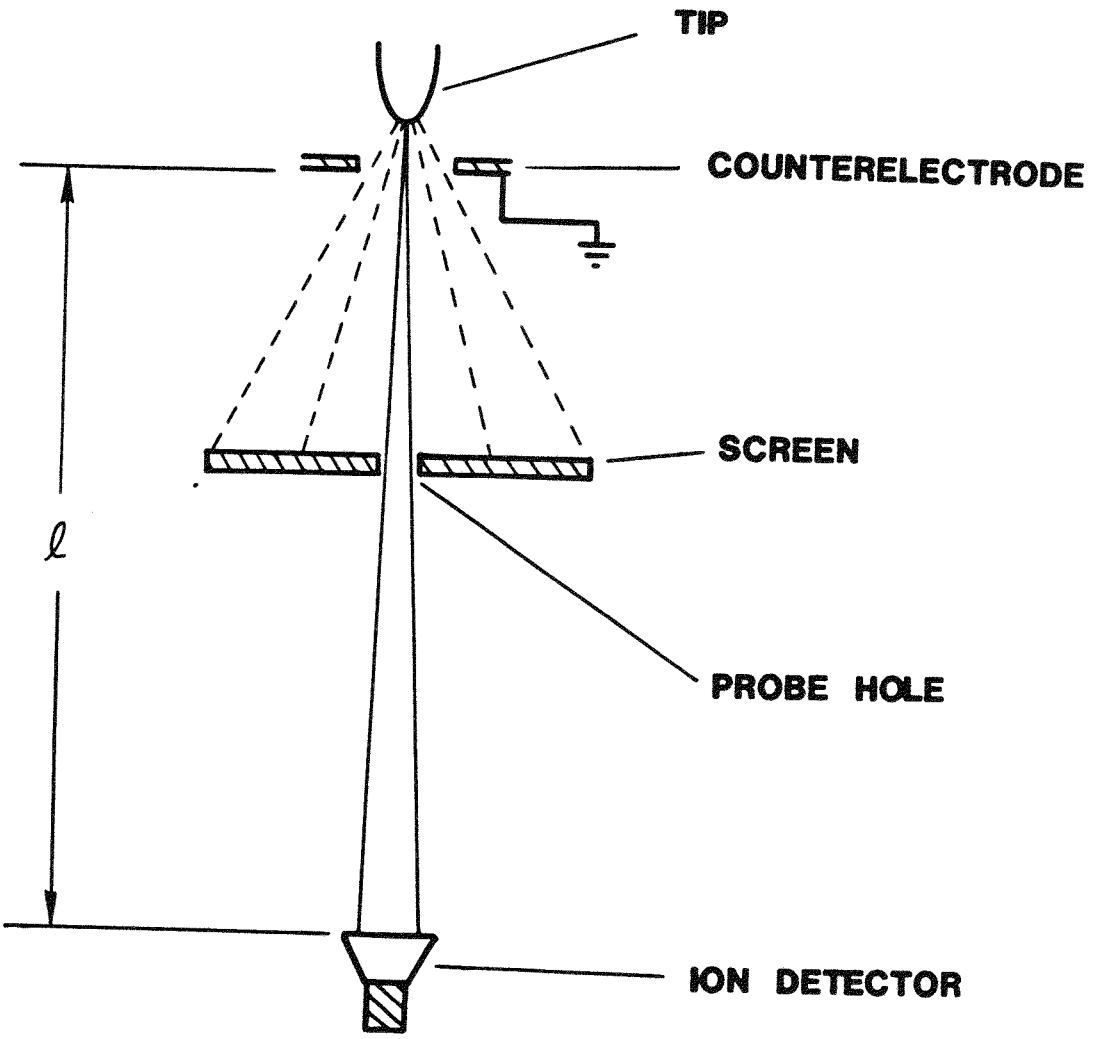

Fig. 5

NUMBER OF IONS
290
220
150
80
0
10
20
30
40
50
60
70
80
90
M/n
O+
Y+++
Cu++
O+2
Cu++
CuO++
Y++
YO++
Cu+
Ba++
CuO+
O2
Cu63
Cu65

Fig. 6

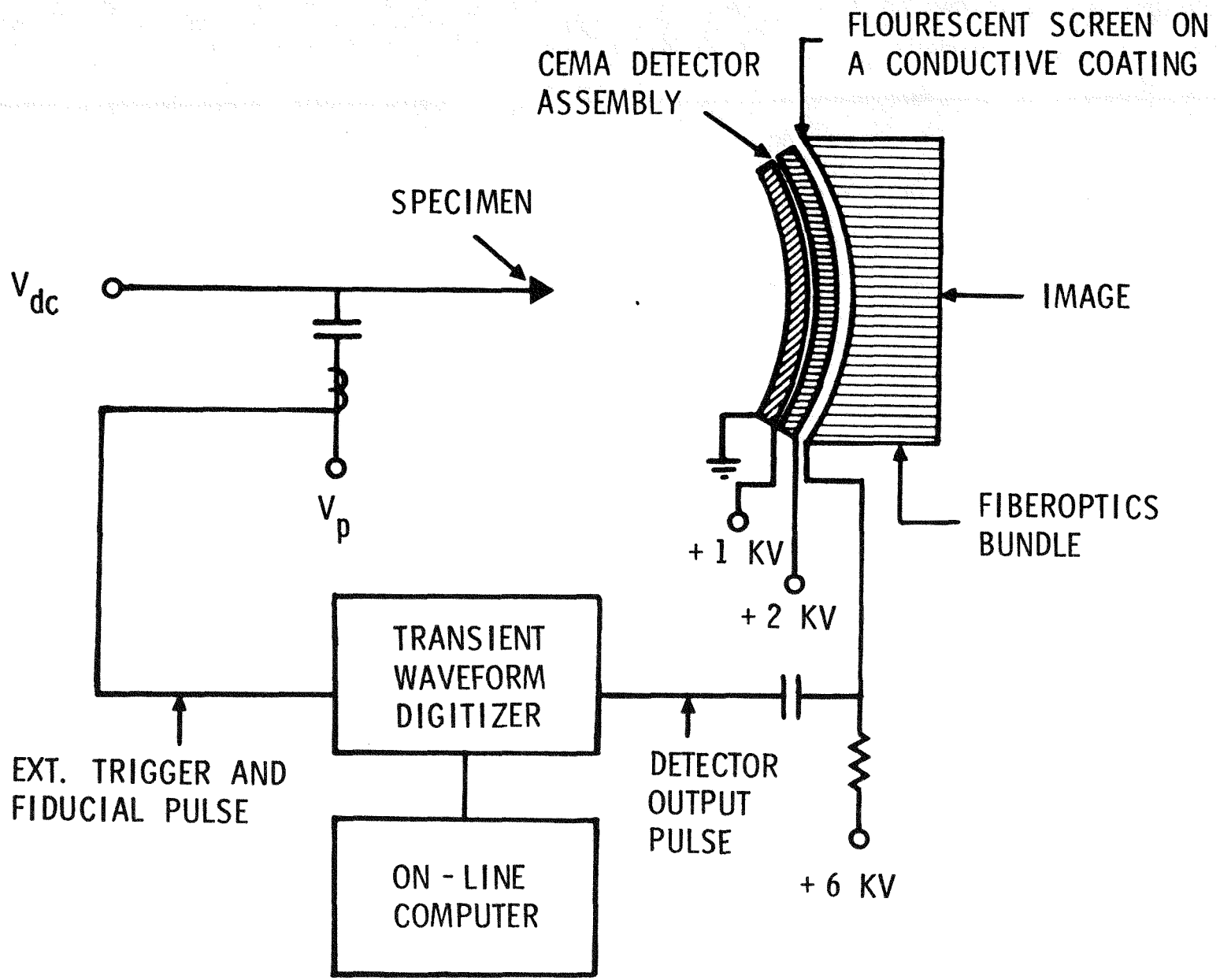
FLOURESCENT SCREEN ON
A CONDUCTIVE COATING
CEMA DETECTOR
ASSEMBLY
SPECIMEN
V_{dc}
IMAGE
V_p
FIBEROPTICS
BUNDLE
+ 1 KV
+ 2 KV
TRANSIENT
WAVEFORM
DIGITIZER
EXT. TRIGGER AND
FIDUCIAL PULSE
DETECTOR
OUTPUT
PULSE
ON - LINE
COMPUTER
+ 6 KV

Fig. 7

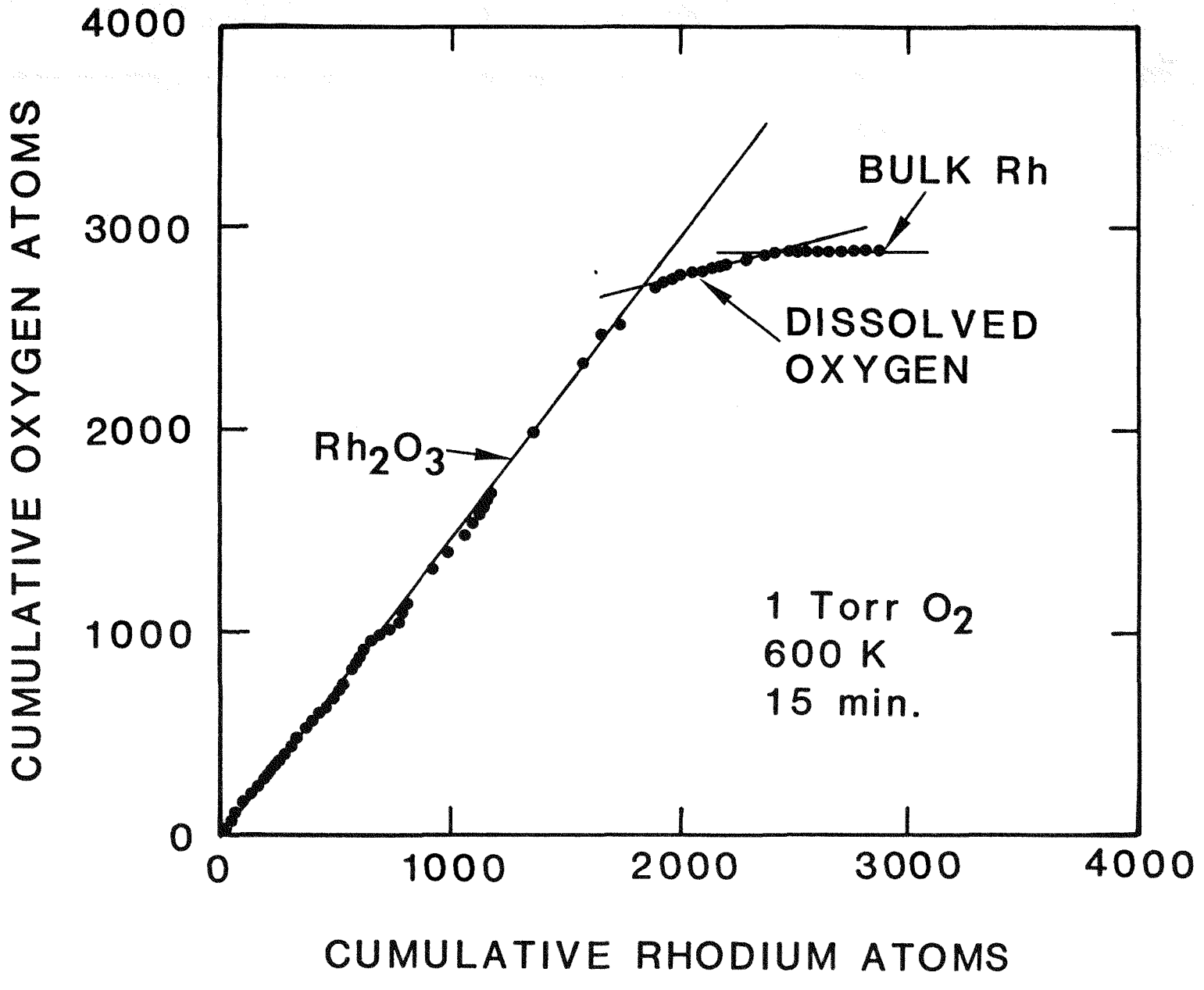
4000
3000
2000
1000
0
0
1000
2000
3000
4000
CUMULATIVE OXYGEN ATOMS
CUMULATIVE RHODIUM ATOMS
BULK Rh
DISSOLVED OXYGEN
Rh_2O_3
1 Torr O_2
600 K
15 min.

8.6.7